Chinese Chemical Letters 35 (2024) 108597

Contents lists available at ScienceDirect

Chinese Chemical Letters

journal homepage: www.elsevier.com/locate/cclet

Synthesis and potential osteogenic applications of Wnt3a-loaded ZIF-8 nanoparticles

Hengfei Wang[a], Song Chen[a,b], Zihan He[a], Junyu Chen[a], Zhou Zhu[a], Qianbing Wan[a], Jian Wang[a,*], Xibo Pei[a,*]

[a] State Key Laboratory of Oral Diseases, National Clinical Research Center for Oral Diseases, Department of Prosthodontics, West China Hospital of Stomatology, Sichuan University, Chengdu 610041, China
[b] Chongqing Key Laboratory of Oral Diseases and Biomedical Sciences, Chongqing Municipal Key Laboratory of Oral Biomedical Engineering of Higher Education, Stomatological Hospital of Chongqing Medical University, Chongqing 400016, China

ARTICLE INFO

Article history:
Received 7 March 2023
Revised 17 May 2023
Accepted 21 May 2023
Available online 23 May 2023

Keywords:
Metal–organic frameworks
Nanoparticle
Drug release
Osteogenesis
Bone defects

ABSTRACT

The Wnt signaling pathway plays a critical role in bone homeostasis, and the related protein therapy strategies have been reported to have great potential in osseointegration; however, they face formidable challenges such as complex external environments and unavoidable protein denaturation. In this work, we report a novel approach combining the synthesis of metal–organic frameworks (MOFs) and protein encapsulation in a one-pot process based on zeolitic imidazolate framework-8 (ZIF-8) and Wnt3a protein, with improved biomechanical behavior and enhanced protein biological response. This combination was designed to enhance the Wnt3a protein function through the improved chemical stability provided by the ZIF-8 crystals. Additionally, the zinc ions contained in the ZIF-8 crystals induced bone homeostasis, further favoring the osteogenesis. The results showed that the Wnt3a protein-loaded ZIF-8 crystals served as efficient drug delivery vehicles to promote osteogenesis, preventing protein denaturation. In particular, Wnt3a-loaded ZIF-8 nanoparticles (Wnt3a@ZIF-8 NPs) had higher efficacy on bone marrow mesenchymal stem cells (BMSCs) than ZIF-8 NPs or Wnt3a proteins, contributing to the osteogenesis through ZIF-8 crystals and intracellular Wnt3a proteins released from Wnt3a@ZIF-8 NPs. Furthermore, polymerase chain reaction (PCR) analysis showed that the osteogenic pathways were upregulated. Overall, the present one-pot process can open up new avenues to develop signaling protein-delivery systems for applications in protein therapy strategies.

In recent years, proteins have emerged as ideal materials, and many studies have demonstrated their positive effect on osteogenesis [1], cancer therapy [2] and immunoregulation [3]. The unique and complex characteristics of osteogenesis have stimulated various studies, and protein-based strategies have attracted gradually increasing interest [4]. For example, it was reported that fibrin proteins have significant effects on the proliferation and differentiation of osteoblasts [5]. Although recombinant proteins have been frequently investigated, their direct use has several disadvantages. First, these proteins are similar to endogenous proteins but have a lower concentration in the body [6], which highlights the significance of delivering recombinant signaling proteins to the intracellular space. In addition, because of the intrinsic properties of most proteins, including their large size, varying surface charges, and fragile tertiary structures, it is hard to deliver target proteins to the intracellular space [7]. Moreover, recombinant proteins can be degraded by proteolytic enzymes, especially in lysosomes [8], and tend to be denatured by oxidation [9]. Therefore, considering the disadvantages of using recombinant proteins alone, it is crucial to design carrier systems for efficient delivery of functional signaling proteins into cells, in order to enhance their effects.

Metal–organic frameworks (MOFs), exhibiting high specific surface area, porosity, and structural diversity [10], have been shown to be good carrier systems for functional signaling proteins [11]. As a member of the MOF family, the zeolitic imidazolate framework-8 nanoparticles (ZIF-8 NPs), bearing zinc ions (Zn^{2+}) as coordination centers, also have excellent biocompatibility and drug-delivery performance [12]. A variety of drugs have been successfully loaded in ZIF-8 NPs. For example, Zheng prepared an anticancer drug system based on ZIF-8 NPs [13], and demonstrated that ZIF-8, serving as a nanocarrier system, could provide a promising platform with good loading rate and controlled release ability. In a previous study

* Corresponding authors.
E-mail addresses: ferowang@hotmail.com (J. Wang), xbpei@hotmail.com (X. Pei).

https://doi.org/10.1016/j.cclet.2023.108597
1001-8417/

[14], Feng prepared proangiogenic miR-21-loaded ZIF-8 NPs and pro-osteogenic miR-5106-loaded ZIF-8 NPs, which achieved lysosomal escape and promoted angiogenesis and osteogenesis. In addition to being good carriers, ZIF-8 NPs also have better application prospect in bone tissue engineering compared with other nanoparticle carrier systems. As previously reported, the canonical mitogen-activated protein kinase (MAPK) signaling pathway plays a key role in osteogenesis under nano-ZIF-8 exposure conditions by phosphorylating extracellular regulated protein kinases (ERK) [15]. The activated MAPK signaling pathway leads to the activation of the osteogenesis-related gene runt-related transcription factor 2 (Runx2), which will alter the proliferation and differentiation of bone marrow mesenchymal stem cells (BMSCs). Similar to MAPK, the Wnt signaling pathway, which can upregulate the gene expression of β-catenin/Runx2, is also crucial for osteogenic differentiation.

The Wnt signaling pathway, as the key to maintaining bone metabolism and homeostasis, is closely related to the osteogenic differentiation of cells and the maintenance of adequate bone mass and density, which play an especially important positive role in fracture healing in systemic diseases such as osteoporosis [16,17]. The Wnt signaling pathway can be influenced by members of the Wnt protein family; for example, the Wnt3a protein, a common activation ligand in the study of Wnt signaling, plays an important role in this pathway, with diverse tissue biological potentials [18]. Helms found that Wnt3a could significantly upregulate the activities of collagen and alkaline phosphatase (ALP) in cells, resulting in osteoid matrix mineralization in surrounding tissues [19]. Furthermore, the binding of Wnt3a protein and its ligand leads to increased phosphorylation of glycogen synthase kinase-3β (GSK-3β), which activates and upregulates the activity through the β-catenin/Runx2/Osterix signaling axis, resulting in significant osteogenic effects [20]. However, it is hard to achieve the best effect with the unprotected Wnt3a protein. On the one hand, it is impossible for Wnt3a, as a typical protein, to avoid lysosomal as well as oxidation stimuli. On the other hand, unescorted Wnt molecules are not easily diffusible in the extracellular milieu because of their high hydrophobicity and tight association with cell membranes [21]. Nevertheless, previous studies of proteins have not explored the potential of ZIF-8 NPs as Wnt3a delivery carriers able to maintain the structural and functional activity of their load for protein therapy.

In this study, Wnt3a@ZIF-8 NPs were designed as stable and biocompatible Wnt3a delivery systems in order to achieve efficient intracellular delivery of Wnt3a protein, activate different signaling pathways, and subsequently achieve high therapeutic performance *in vitro*. In this combination, ZIF-8 crystals can improve the function of Wnt3a protein, and the latter works together with zinc ions. Compared with serum albumin, metallic, and organic nanoparticles [22–24], Wnt3a@ZIF-8 NPs have better biocompatibility and more stable physicochemical properties. Additionally, in this combination, zinc ions and Wnt3a protein can promote osteogenesis. Therefore, we first prepared Wnt3a@ZIF-8 NPs *via* one-pot synthesis and investigated their characteristics. Then, their effects on cell behavior were studied by focusing on osteogenic differentiation *in vitro*, and a series of experiments were performed to elucidate the related intracellular pathways. Overall, this study explored the biological properties and osteoinductive mechanisms of Wnt3a@ZIF-8 NPs and provided an effective basis for the preparation of signaling protein-loaded carrier systems for bone tissue regeneration.

In order to study the phase purity of Wnt3a@ZIF-8 nanoparticles, the crystals in the mother solution used for the synthesis of these NPs were collected and analyzed by scanning electron microscopy (SEM), transmission electron microscopy (TEM), Fourier transform infrared spectroscopy (FT-IR), X-ray diffraction (XRD), X-ray photoelectron spectroscopy (XPS), thermogravimetric analysis (TGA), and zeta potential measurements, which were compared with those of ZIF-8 or Wnt3a.

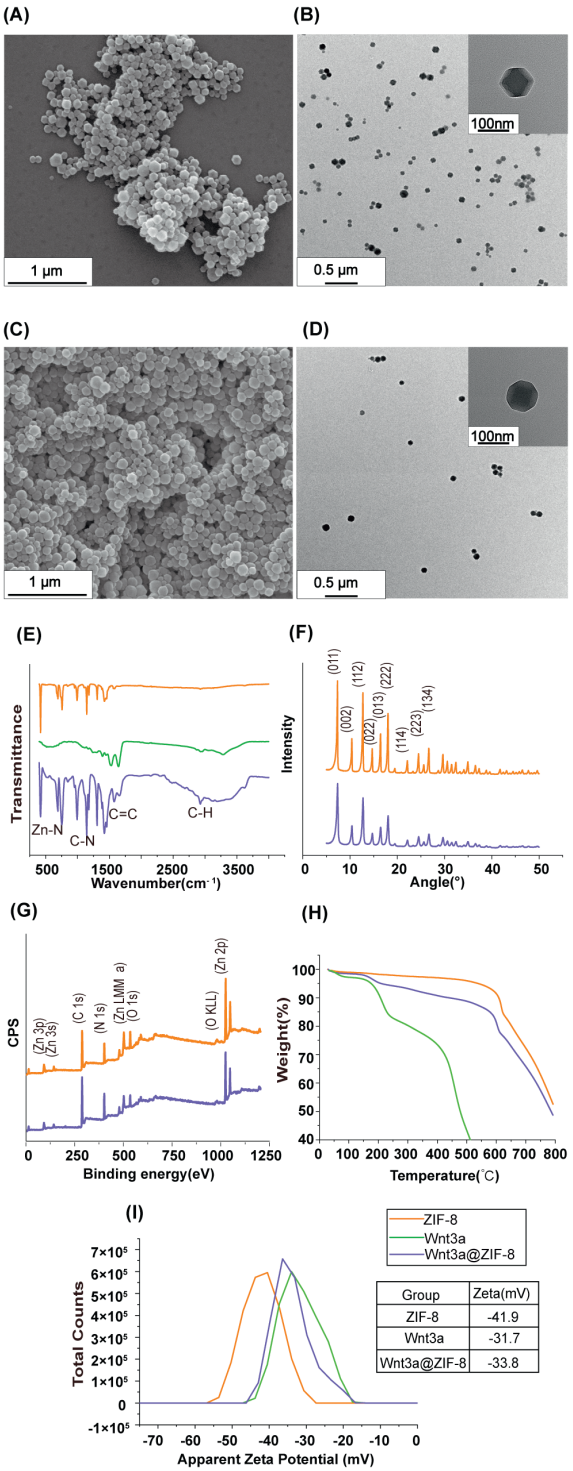

Fig. 1. Characterization of ZIF-8 and Wnt3a@ZIF-8 NPs. SEM (A) and TEM (B) images of ZIF-8 NPs; SEM (C) and TEM (D) images of Wnt3a@ZIF-8 NPs; (E) FT-IR spectra of ZIF-8 NPs, Wnt3a, and Wnt3a@ZIF-8 NPs; (F) XRD patterns of ZIF-8 and Wnt3a@ZIF-8 NPs; (G) XPS spectra of ZIF-8 NPs and Wnt3a@ZIF-8 NPs; (H) TGA profile of ZIF-8 NPs, Wnt3a, and Wnt3a@ZIF-8 NPs; (I) zeta potentials of ZIF-8 NPs, Wnt3a, and Wnt3a@ZIF-8 NPs.

Considering that Wnt3a protein is not a MOF and mainly consists of C, H, O, and N elements that have a small influence on the XPS profiles of ZIF-8 and Wnt3a@ZIF-8, Wnt3a was not identified by XRD and XPS. The SEM and TEM images in Figs. 1A and B show

that the typical ZIF-8 NPs had monodispersed dodecahedron structures with diameters of 71–90 nm (Fig. S1A in Supporting information). Compared with the synthesized Wnt3a@ZIF-8 NPs (Figs. 1C and D), with most diameters ranging from 91 nm to 110 nm (Fig. S1B in Supporting information), the Wnt3a@ZIF-8 NPs were more homogeneous in size, which might be due to the presence of Wnt3a. However, previous studies found that loading proteins led to irregular sizes [25]. This discrepancy might be due to the different synthesis methods used for ZIF-8 NPs and Wnt3a@ZIF-8 NPs, especially in terms of different reaction times. Additionally, the Wnt3a@ZIF-8 NPs exhibited a rounder shape, which was probably related to the presence of Wnt3a.

The FT-IR spectra of ZIF-8 and Wnt3a@ZIF-8 NPs in Fig. 1E show many similar characteristic peaks. The absorption band between 250 and 4000 cm^{-1}, due to the stretching vibration of C-H, C=C, C-N, and Zn-N bonds, was observed for both ZIF-8 and Wnt3a@ZIF-8 NPs. The main peaks of Wnt3a (C=C and C-H) were also found for Wnt3a@ZIF-8 NPs, which confirmed that Wnt3a was successfully loaded in ZIF-8. Although the loading of Wnt3a was confirmed, it did not influence the characteristic peaks of ZIF-8. The XRD patterns (Fig. 1F) provided additional evidence of the successful formation of Wnt3a@ZIF-8 NPs, showing that the crystal structure of Wnt3a@ZIF-8 NPs was similar to that of ZIF-8 NPs, and the loading of Wnt3a did not change the phase purity of the synthesized nanoparticles. This result was further confirmed by the XPS profiles of ZIF-8 and Wnt3a@ZIF-8 NPs in Fig. 1G, which showed no obvious differences in the chemical elements present in both samples. The results in Fig. 1H confirmed the presence of Wnt3a by comparing the TGA curves of three groups (ZIF-8, Wnt3a and Wnt3a@ZIF-8); moreover, both ZIF-8 and Wnt3a@ZIF-8 NPs showed good thermostability. In particular, the weight loss of the Wnt3a group was higher than that of Wnt3a@ZIF-8 and ZIF-8 NPs at each time point as the temperature was increased from 0 °C to 800 °C (Fig. S1C in Supporting information). As an efficient drug carrier and thermostable shell, ZIF-8 crystals clearly affected the thermostability of Wnt3a protein; in other words, the synthesis of Wnt3a@ZIF-8 NPs enhanced the stability of Wnt3a protein in terms of material characteristics. In addition, the zeta potentials of ZIF-8 NPs, Wnt3a, and Wnt3a@ZIF-8 NPs were calculated separately. A previous study showed that the zeta potential of the nanoparticles could affect the properties of nanodrug delivery system, and values around −40 mV were acceptable in terms of biocompatibility [26]. Furthermore, it has been reported that nanoparticles with a neutral surface charge may exhibit superior biocompatibility [27]. The Wnt3a protein resulted in a slight change in zeta potential from −41.9 mV to −33.8 mV (Fig. 1I), which improved the biocompatibility of the ZIF-8 NPs.

For the purpose of identifying the best way to synthesize Wnt3a@ZIF-8 NPs, five groups were designed to determine the proportion of Wnt3a protein in Wnt3a@ZIF-8 NPs by comparing their surface morphology based on SEM. Peng synthesized hemoglobin (HB)@ZIF-8 to improve the stability of free hemoglobin and reported that the polydispersity index of the particle size changed when different concentrations of HB were used [25]. Similarly, as shown in Fig. S1D (Supporting information), when the protein dosage exceeded 500 μg, the synthesized Wnt3a@ZIF-8 NPs became heterogeneous and unstable, which was attributed to their protein content.

Considering that the surface morphology and shape of crystalline nanostructures govern their biocompatibility and a further increase in inhomogeneity may induce necrosis [28], the protein dosage was chosen to be 500 μg in order to obtain a better morphology and load a higher protein amount. In addition, the encapsulation efficiency of Wnt3a@ZIF-8 NPs was found to be 91.8%, and the release dynamics of Wnt3a@ZIF-8 NPs were shown to remain low (Fig. S2 in Supporting information).

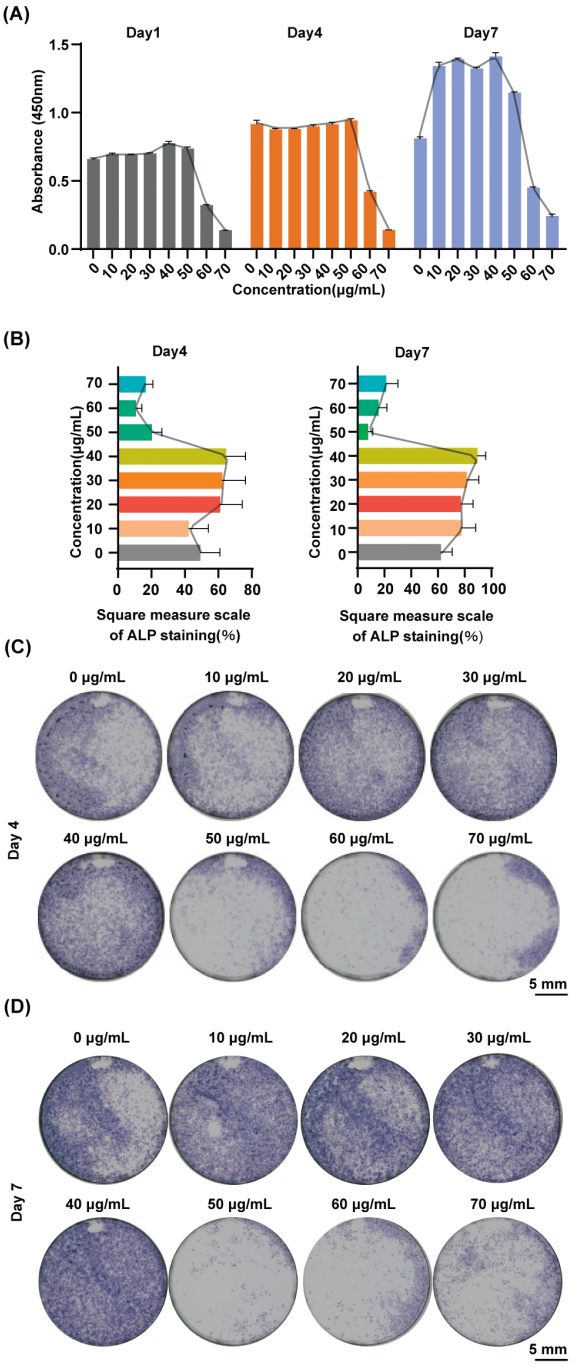

Fig. 2. Optimization of concentration of Wnt3a@ZIF-8 NPs. CCK-8 assays (A) of BMSCs cultured in normal culture medium. ALP activity (B) of BMSCs cultured in osteogenic induction medium and treated with different concentrations of Wnt3a@ZIF-8 NPs. ALP staining of BMSCs in osteogenic induction medium cultured with different concentrations of Wnt3a@ZIF-8 NPs for 4 days (C) and 7 days (D). The data were analyzed by the mean ± standard deviation (SD). (n=3).

To investigate the biocompatibility of the nanoparticles, the cell counting kit-8 (CCK-8) assay (Fig. 2A) was used to monitor the proliferation of BMSCs in normal culture medium. For Wnt3a@ZIF-8 NPs, there was no significant difference among the different concentration groups on day 1, except for the 60 and 70 μg/mL groups. After 4 days of culture, similar results were found among the groups from 0 to 50 μg/mL. After 7 days of culture, the proliferations of BMSCs in the 10, 20, 30, 40, and 50 μg/mL groups were higher than that in the blank group. Furthermore, ZIF-8 NPs were

subjected to the same analysis in Fig. S4 (Supporting information) and similar curves were obtained. Therefore, the loading of Wnt3a protein into ZIF-8 crystals had no negative effect on the cell proliferation; in fact, the loading of Wnt3a protein resulted in a greater contribution to the growth of BMSCs compared with that observed for ZIF-8 NPs. In addition, in order to determine the appropriate concentrations of ZIF-8 and Wnt3a@ZIF-8 NPs for osteogenesis, BMSCs were cultured in osteogenic induction medium and ALP staining was performed to measure the partial osteogenesis characteristics of BMSCs on days 4 and 7 (Figs. 2C and D). As shown in Fig. 2C, a deeper ALP color was observed as long as the concentration was below 40 μg/mL. A similar trend was observed in Fig. 2D. As shown in Fig. 2B, the ALP staining of BMSCs from 10 μg/mL to 40 μg/mL was larger than that in the blank group, and the 40 μg/mL group seemed to reach a peak on days 4 and 7, which further confirmed the differentiation of BMSCs. Therefore, the 40 μg/mL concentration was chosen for the follow-up experiments on the ZIF-8, bovine serum albumin (BSA)-loaded ZIF-8 nanoparticles (BSA@ZIF-8), and Wnt3a@ZIF-8 groups. In the case of the Wnt3a group, considering that the encapsulation efficiency of Wnt3a in Wnt3a@ZIF-8 NPs was 91.8%, the concentration of Wnt3a for the follow-up experiments was chosen to be 0.0612 μg/mL. The similar results obtained for the ZIF-8 and Wnt3a@ZIF-8 groups in the concentration optimization experiments were related to their similar chemical structures and, especially, similar zinc ion releases. We also confirmed that high concentrations of zinc ions were detrimental to cell growth. In addition, Fig. S5 (Supporting information) illustrates the good biocompatibility of the different groups in different environments.

As shown in a previous study, cell adhesion is a very important cell–material interaction [29]. Especially for mesenchymal stem cells (MSCs), adhesion and morphology are fundamental for migration, proliferation, and differentiation [30]. In this study, the initial cell adhesion on cell culture plate surfaces was investigated by fluoresceine isothiocyanate (FITC)-phalloidin and 4′,6-diamidino-2′-phenylindole (DAPI) staining, in order to reveal β-actin and nuclei, respectively. After 24 h of culture, the BMSCs cultured on plates were stable, and active lamellipodium protrusions with polygonal shape were observed for the cells in each group, same as for the blank group (Fig. 3A); this also showed that 40 μg/mL concentrations of several groups (0.0612 μg/mL for Wnt3a) had no negative effect on cell adhesion. Endocytosis tests were performed to confirm that Wnt3a@ZIF-8 NPs were internalized by endocytosis and the Wnt3a signaling protein was loaded inside BMSCs. Fig. 3B shows that Wnt3a@ZIF-8 NPs were successfully transported across the cytomembrane. In a previous study, Gao confirmed that ZIF-8 NPs were transported through the cytomembrane by translocation [12]. The results of this study show that Wnt3a@ZIF-8 NPs also gained entry into the cells after 3 h, similar to ZIF-8 NPs.

In addition, the dynamic changes in cell proliferation and apoptosis (Fig. 3C) were consistent with the above results (Fig. S5A in Supporting information). Cell apoptosis is an important proliferation-related process in cell physiology. There is no doubt that the rate of cell proliferation should be greater than that of cell apoptosis during bone formation. Calcein acetoxymethyl ester/propidium iodide (calcein AM/PI) staining was conducted to investigate the cell apoptosis of five groups. AM-stained viable cells and PI-stained dead cells emitted green and red fluorescence, respectively. After 24 h (Fig. 3C) and 72 h (Fig. 3D) of culture, the BMSCs underwent proliferation and apoptosis, as revealed by the ratio between green and red fluorescence. The green/red ratios in the ZIF-8 and Wnt3a groups exhibited a significant increase compared with the blank group after 24 h (Fig. 3E). Although no significant difference was observed with the control group, the BSA@ZIF-8 and Wnt3a@ZIF-8 groups showed better results in terms of dynamic proliferation. Different results were found after 72 h, with

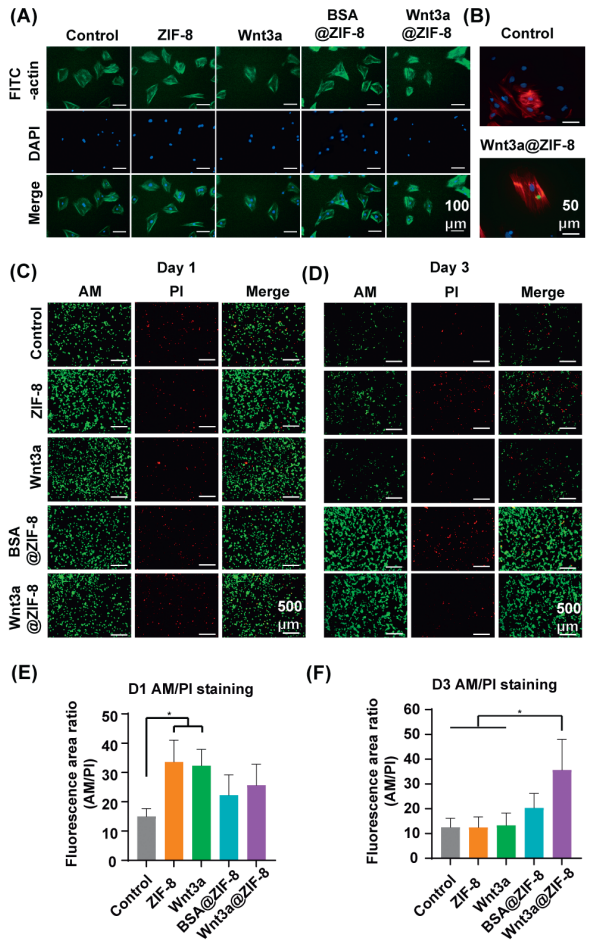

Fig. 3. Fluorescent staining of different groups. Cell nuclei and β-actins (A) of BMSCs cultured in normal culture medium and treated in different groups for 1 day. Cell nuclei marked by DAPI were blue and actins marked by FITC were green. Endocytosis (B) of BMSCs treated with PBS and FITC-Wnt3a@ZIF-8 NPs in normal culture medium for 3 h. Cell nuclei marked by DAPI were blue, actins marked by rhodamine were red, and FITC-Wnt3a@ZIF-8 NPs were green. Calcein AM/PI cell viability assay of BMSCs cultured in normal culture medium for 1 day (C) and 3 days (D). Fluorescence intensity of calcein AM/PI cell viability assay calculated and divided by day 1 (E) and day 3 (F). The data were analyzed by the mean ± SD (n=3. $^*P < 0.05$ between each group).

the Wnt3a@ZIF-8 group showing higher cell proliferation (Fig. 3F). In summary, positive dynamic proliferations were observed for the four groups compared with the control group, and the Wnt3a@ZIF-8 NPs were found to be beneficial to cell proliferation. In particular, the Wnt3a signaling protein had a positive effect on early cell proliferation and its effect declined with time, which might be due to its inactivation. Similarly, although the ratio of proliferation and apoptosis in the ZIF-8 group was higher than that in the blank group after 24 h, no significant difference was observed after 72 h, which might be related to the positive effect of metal ions.

A large amount of metal ions is related to the production of reactive oxygen species (ROS). Some studies indicated that the toxicity of high concentration of ZIF-8 NPs might originate from the promoted production of ROS in mitochondria and the high level of oxidative stress due to zinc ions [31]. However, some studies suggested that low concentrations of zinc ions could promote a significant improvement of cell viabilities and play a role in superoxide dismutases (SODs) [32]. Therefore, zinc ions play a key role in maintaining the balance of the organism. Reducing the concentration of ROS contributed to cell growth and function. Based on the

results of BMSC proliferation tests in normal media, a 24 h culture time was chosen for the ROS investigation to eliminate differences caused by proliferation. As shown in Figs. S6A and B (Supporting information), the production of ROS in the ZIF-8 NPs group was lower than that in the blank group, which might be due to the slow release of zinc ions. The different production of ROS by ZIF-8 and Wnt3a@ZIF-8 groups might result from the faster release of zinc ions in Wnt3a@ZIF-8 NPs from 12 h to 24 h. The lower ROS concentration in the ZIF-8 group could explain the difference with the control group (Fig. 3E). However, although the ROS productions in the BSA@ZIF-8 and Wnt3a@ZIF-8 groups were higher than that in the ZIF-8 group, there was no significant difference compared with the control group (Fig. S6B). Similar results are shown in Fig. 3E, and the Wnt3a@ZIF-8 NPs also exhibited good biocompatibility.

Bone reconstruction is a complex and slow process, which requires cell viability, an appropriate internal environment, effective calcium deposits, and a stable location [33]. ALP can generate inorganic phosphate species and promote calcium phosphate deposition [34]. The main constituent of vertebrate bones is calcium phosphate/hydroxyapatite (HA), and effective calcium deposits are crucial for bone formation [35]. Collagen plays a role in providing special functions as a scaffold structure for cell migration, proliferation, and secretion at the same time [36]. In addition, collagen mineralization is an important biological process in skeletal tissues [37]. To evaluate the osteogenic activity of Wnt3a@ZIF-8 NPs at the molecular level, in this study we investigated the secretion of ALP protein, calcium nodules, and collagen as well as the expression of osteogenic-related genes [Runx2, osteopontin (Opn), Alp, and osteocalcin (Ocn)] [38].

ALP protein, an early osteogenic marker, is mainly distributed in cassette transporters on the cytomembrane. Its high activity denotes osteoblast growth and differentiation [39]. Therefore, 4 and 7 days were chosen to confirm the changes in early bone formation. In the ALP staining assay, the ALP protein was stained blue [40]. No significant difference was found after 4 days of culture (Fig. 4A) or after calculating the square measure scale of stained cells (Fig. 4C). However, significant differences were observed after 7 days (Fig. 4B). The statistical analysis of the images (Fig. 4D) shows that four groups (ZIF-8, Wnt3a, BSA@ZIF-8, and Wnt3a@ZIF-8) had higher ALP activity than control group. No significant difference was found among the four groups, because the deep color reaction produced by the catalytic reaction of ALP to nitroblue tetrazolium chloride (NBT) and 5–bromo-4–chloro-3-indolyl phosphate (BCIP) made it hard to visually separate light from shaded regions.

Moreover, the ALP activity was confirmed by quantitative analysis. As displayed in Fig. 4E, after 4 days of culture, the ALP activities of BMSCs treated in different groups showed no significant differences, which was due to the production cycle of BMSCs. After 7 days, the ALP activity of BMSCs treated with Wnt3a@ZIF-8 NPs was significantly higher than that of the cells in the control group, which confirmed that Wnt3a@ZIF-8 could play a role in the osteogenic activity; however, no significant difference was found between the blank group and other groups. After 14 days, the ALP activity of BMSCs treated with ZIF-8 NPs, BSA@ZIF-8 NPs, and Wnt3a@ZIF-8 NPs was significantly higher than that of the control group, which confirmed that different nanoparticles and Wnt3a signaling proteins could enhance the ALP activity at the cellular level, as reported in other studies. The difference between the control and Wnt3a groups revealed that the Wnt3a signaling protein could play a role in the ALP activity. The absence of significant differences between ZIF-8 and BSA@ZIF-8 groups showed that BSA, as a basic synthetic material, had a small influence on the activity of ZIF-8 NPs. In addition, compared with the Wnt3a and BSA@ZIF-8 groups, the Wnt3a@ZIF-8 group revealed that the Wnt3a signaling protein delivered by ZIF-8 yielded better results in terms of ALP activity.

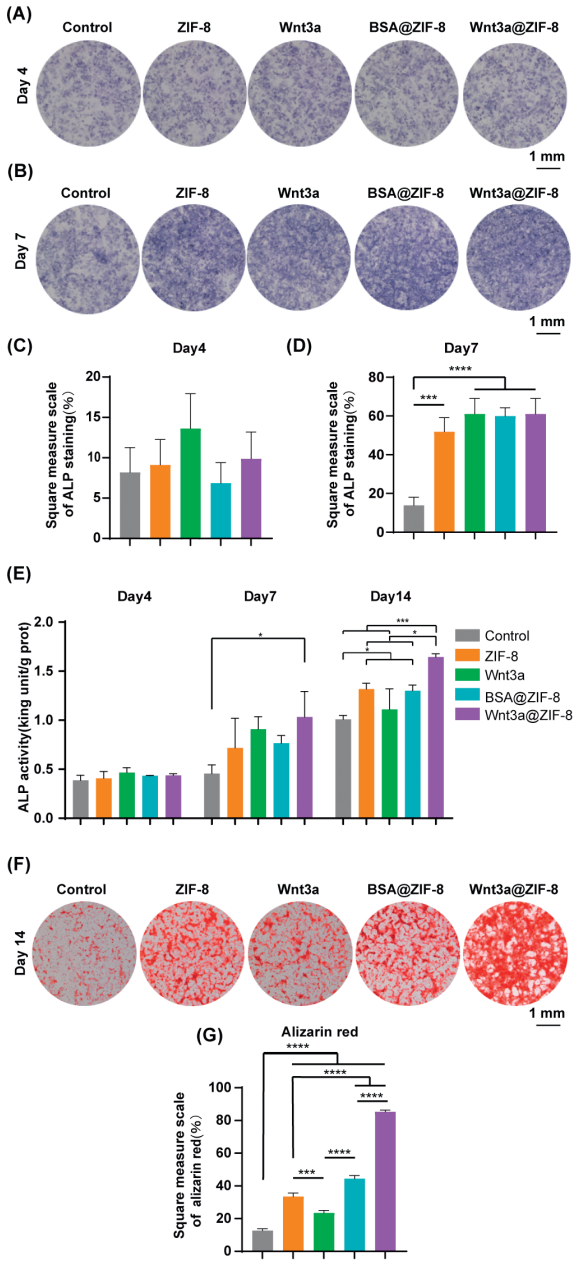

Fig. 4. Microscopic analysis of osteogenesis of different groups in terms of ALP and calcium nodules. ALP staining of BMSCs treated in different groups for 4 days (A) and 7 days (B) along with corresponding calculated square measure scales (C, D). ALP activity assay (E) of BMSCs treated in different groups for 4, 7 and 14 days. Alizarin red staining (F) of BMSCs treated in different groups for 14 days and calculated square measure scales (G). The data were analyzed by the mean ± SD (n=3. $^{*}P < 0.05$, $^{***}P < 0.001$, and $^{****}P < 0.0001$ between each group).

Effective calcium nodule deposition is also significant during osteogenic differentiation. Calcium deposits, a later osteogenesis marker, can be identified as red spots after Alizarin red staining [41]. As displayed in Figs. 4F and G, after 14 days of culture, the quantity of calcium nodule deposits of BMSCs treated with Wnt3a@ZIF-8 NPs was higher than that of the cells treated with phosphate buffered saline (PBS), ZIF-8 NPs, Wnt3a, and BSA@ZIF-8 NPs; this revealed that the Wnt3a@ZIF-8 NPs had a positive effect on the production of calcium nodules. Previous studies confirmed that ZIF-8 NPs contributed to calcium nodule deposition, as also observed in this work. The calcium nodule deposition of the Wnt3a group was only higher than that of the control group,

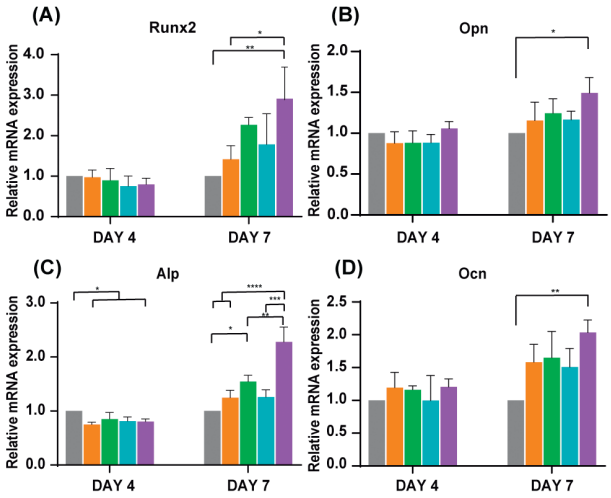

Fig. 5. Osteogenesis of different groups in terms of related gene expressions. The mRNA expression of Runx2 (A), Opn (B), Alp (C), and Ocn (D) in different groups. The data were analysed by the mean ± SD (n=3. $^{*}P < 0.05$, $^{**}P < 0.01$, $^{***}P < 0.001$, and $^{****}P < 0.0001$ between each group).

which might be due to the inactivation of the Wnt3a signaling protein outside the BMSCs during long-term culture. Moreover, the Wnt3a signaling protein was undoubtedly protected until its activation in the cells. The production of collagen was also confirmed in Fig. S7 (Supporting information).

In terms of ALP activity, calcium nodule deposition, and collagenation, ZIF-8 revealed its advantage as a delivery system of Wnt3a signaling protein, and Wnt3a@ZIF-8 NPs produced better results than ZIF-8 NPs, Wnt3a protein, and BSA@ZIF-8 NPs. Wnt3a@ZIF-8 NPs showed good osteogenic effects in an *in vitro* osteogenic-related assay.

Furthermore, the mRNA expressions of osteogenesis-related genes (Runx2, Opn, Alp, and Ocn) were measured by quantitative polymerase chain reaction (q-PCR) after culturing for 4 and 7 days (Fig. 5). There was no significant difference in Runx2, Opn, Ocn expression and slight decline in Alp expression among the five groups on day 4, which might result from cell viability and did not have obvious influence on the secretion of ALP according to Figs. 4A-E. However, significant differences were observed at a later stage (day 7). Runx2 has multiple functions in skeletal development, including osteoblast differentiation, proliferation of osteoblast progenitors, and matrix protein gene expression in osteoblasts [42]. As shown in Fig. 5A, significant differences were found between the Wnt3a@ZIF-8 group and the control as well as ZIF-8 groups. The Runx2 expression is necessary for osteoblast differentiation and can promote the expression of Opn, Alp, and Ocn [43], which was also confirmed by Figs. 5B–D. Opn, as a glycosylated protein, is widely localized in the extracellular matrix and participates in a host of cellular activities such as migration, adhesion, differentiation, and survival [44]. As shown in Fig. 5B, a high Opn expression was found in the Wnt3a@ZIF-8 group. Fig. 5C shows that the Wnt3a and Wnt3a@ZIF-8 groups achieved better results in terms of Alp expression than the control group. In addition, the Wnt3a@ZIF-8 NPs had a stronger effect than ZIF-8 and BSA@ZIF-8 NPs on the expression of Alp. In terms of Ocn (another osteogenesis-related gene) expression, Fig. 5D shows similar results for the Wnt3a@ZIF-8 and control groups, as in Fig. 5A.

In this work, Wnt3a protein was successfully loaded into ZIF-8 NPs, and the obtained Wnt3a@ZIF-8 showed enhanced osteogenic activity compared to control, ZIF-8, Wnt3a, and BSA@ZIF-8 groups. SEM, TEM, FTIR, XRD, XPS, TGA and zeta potential measurements confirmed that Wnt3a@ZIF-8 NPs were synthesized successfully. In addition, zinc ions could be slowly released from Wnt3a@ZIF-8 NPs in a similar way to ZIF-8 NPs. *In vitro* experiments revealed that the introduction of Wnt3a into ZIF-8 NPs had a positive effect on the osteogenesis of BMSCs, and ZIF-8 NPs, as good carriers, successfully maintained the activity of the Wnt3a protein. Similar to ZIF-8 NPs, the Wnt3a@ZIF-8 NPs were biocompatible with BMSCs and hemocytes, and could promote the secretion of osteogenesis-related proteins (ALP) and genes (Runx2, Opn, Alp, and Ocn). Moreover, the productions of calcium deposits and collagen induced by Wnt3a@ZIF-8 NPs were significantly higher than that induced in the blank and ZIF-8 groups, which highlighted the great potential of the Wnt3a@ZIF-8 NPs in osteogenesis. In conclusion, Wnt3a@ZIF-8 NPs showed great biocompatibility as well as higher osteogenic activity, suggesting that they could promote bone formation; moreover, using ZIF-8 NPs as carriers would be a promising strategy for delivering signaling proteins.

Declaration of competing interest

We declare that we have no financial and personal relationships with other people or organizations that can inappropriately influence our work, there is no professional or other personal interest of any nature or kind in any product, service and/or company that could be construed as influencing the position presented in, or the review of, the manuscript entitled.

Acknowledgments

This work was financially supported by National Nature Science Foundations of China (Nos. 82271016, 82271034, 82270961, 82071164, 8197032972, 81901060), Key research program of Sichuan Science and technology Department (No. 2021YFS0052), Research and Development Program (West China Hospital of Stomatology, Sichuan University) (Nos. RD-03-202107, RD-03-202310).

Supplementary materials

Supplementary material associated with this article can be found, in the online version, at doi:10.1016/j.cclet.2023.108597.

References

[1] L.R. Lee, A.E. Holman, X. Li, et al., Bone 159 (2022) 116378.
[2] Q. Zhang, J. Zhang, J. Song, et al., ACS Nano 15 (2021) 8001–8038.
[3] Y. Su, Y. Gu, R. Wu, H. Wang, Stem Cells Int. 2018 (2018) 9837035.
[4] M. Botor, A. Fus-Kujawa, M. Uroczynska, et al., Biomolecules 11 (2021) 1493.
[5] J.H. Oh, H.J. Kim, T.I. Kim, K.M. Woo, BMB Rep. 47 (2014) 110–114.
[6] B.T. Griffin, J. Guo, E. Presas, et al., Adv. Drug Deliv. Rev. 106 (2016) 367–380.
[7] N. Chen, Y. He, M. Zang, et al., Biomaterials 286 (2022) 121567.
[8] A. Ballabio, J.S. Bonifacino, Nat. Rev. Mol. Cell Biol. 21 (2019) 101–118.
[9] C.A. Juan, J.M. Pérez de la Lastra, F.J. Plou, E. Pérez-Lebeña, Int. J. Mol. Sci. 22 (2021) 4642.
[10] J. Zhuang, C.H. Kuo, L.Y. Chou, et al., ACS Nano 8 (2014) 2812–2819.
[11] M. Velasquez, E. Astria, S. Winkler, et al., Chem. Sci. 11 (2020) 1835–1843.
[12] X. Gao, Y. Xue, Z. Zhu, et al., ACS Appl. Mater. Interfaces 13 (2020) 97–111.
[13] H. Zheng, Y. Zhang, L. Liu, et al., J. Am. Chem. Soc. 138 (2016) 962–968.
[14] H. Feng, Z. Li, W. Xie, et al., Chem. Eng. J. 430 (2022) 132867.
[15] J. Ran, C. Ma, K. Xu, et al., Drug Des. Dev. Ther. 12 (2018) 1195–1204.
[16] Y. Okuchi, J. Reeves, S.S. Ng, et al., Nat. Mater. 20 (2020) 108–118.
[17] L. Yu, T. Gao, W. Li, et al., Bioact. Mater. 20 (2023) 598–609.
[18] T.N. Volleman, J. Schol, K. Morita, D. Sakai, M. Watanabe, Neurospine 17 (2020) 19–35.
[19] A. Popelut, S.M. Rooker, P. Leucht, et al., Biomaterials 31 (2010) 9173–9181.
[20] J. Wang, J. Yang, X. Cheng, et al., J. Agric. Food Chem. 67 (2019) 10285–10295.
[21] C. Korkut, B. Ataman, P. Ramachandran, et al., Cell 139 (2009) 393–404.
[22] Y. Wang, S. Chen, X. Yang, S. Zhang, C. Cui, Drug Des, Dev. Ther. 15 (2021) 1531–1547.
[23] R. Crovador, H. Heim, S. Cottam, et al., ACS Appl. Bio Mater. 4 (2021) 6338–6350.
[24] R. Eivazzadeh-Keihan, E. Bahojb Noruzi, K.Khanmohammadi Chenab, et al., J. Tissue Eng. Regen. Med. 14 (2020) 1687–1714.
[25] S. Peng, J. Liu, Y. Qin, et al., ACS Appl. Mater. Interfaces 11 (2019) 35604–35612.
[26] Y. Song, H. Li, F. Lu, et al., J. Mater. Chem. B 5 (2017) 6008–6015.

[27] S. Peng, Y. Men, R. Xie, Y. Tian, W. Yang, J. Colloid. Interface Sci. 539 (2019) 19–29.
[28] Z. Ou, L. Yao, H. An, B. Shen, Q. Chen, Nat. Commun. 11 (2020) 4555.
[29] Y. Zhuang, C. Zhang, M. Cheng, et al., Bioact. Mater. 6 (2021) 1791–1809.
[30] L. Yang, Q. Gao, L. Ge, et al., Biomater. Sci. 8 (2020) 2638–2652.
[31] B. Liu, Y. Yang, H. Wu, et al., Small 19 (2023) 2205682.
[32] G.K. Jakubiak, K. Osadnik, M. Lejawa, et al., Antioxidants 11 (2021) 79.
[33] H. Ping, W. Wagermaier, N. Horbelt, et al., Science 376 (2022) 188–192.
[34] K. Zhang, Z. Jia, B. Yang, et al., Adv. Sci. 5 (2018) 1800875.
[35] Y. Chen, R. Koshy, E. Guirado, A. George, Acta Biomater. 120 (2021) 224–239.
[36] G.A. Rico-Llanos, S. Borrego-González, M. Moncayo-Donoso, J. Becerra, R. Visser, Polymers 13 (2021) 599.
[37] B.M. Oosterlaken, M.P. Vena, G. de With, Adv Mater. 33 (2021) 2004418.
[38] Z. Zhang, B. Jia, H. Yang, et al., Biomaterials 275 (2021) 120905.
[39] G. Shen, H. Ren, Q. Shang, et al., EBioMedicine 52 (2020) 102626.
[40] C. Xu, Y. Kang, X. Dong, D. Jiang, M. Qi, Chin. Chem. Lett. 34 (2023) 107528.
[41] P. Pan, X. Chen, H. Xing, et al., Chin. Chem. Lett. 32 (2021) 2159–2163.
[42] J.M. Kim, Y.S. Yang, K.H. Park, et al., Nat. Commun. 11 (2020) 2289.
[43] J.S. Lee, J.M. Lee, G.I. Im, Biomaterials 32 (2011) 760–768.
[44] X. Pang, K. Gong, X. Zhang, et al., Pharmacol. Res. 144 (2019) 235–244.